Acta Pharmacologica Sinica

www.nature.com/aps

ARTICLE

Exogenous glutathione exerts a therapeutic effect in ischemic stroke rats by interacting with intrastriatal dopamine

He Wang[1], Yi-sha Du[1], Wen-shuo Xu[1], Chang-jian Li[1], Hong Sun[1], Kang-rui Hu[1], Yuan-zhuo Hu[2], Teng-jie Yu[1], Hui-min Guo[1], Lin Xie[1], Guang-ji Wang[1] and Yan Liang[1]

We previously showed that oral administration of exogenous glutathione (GSH) exerted a direct and/or indirect therapeutic effect on ischemic stroke rats, but the underlying mechanisms remain elusive. In the current study, we conducted a quantitative proteomic analysis to explore the pathways mediating the therapeutic effect of GSH in cerebral ischemia/reperfusion (I/R) model rats. Rats were subjected to middle cerebral artery occlusion (MCAO) for 2 h followed by reperfusion. The rats were treated with GSH (250 mg/kg, ig) or levodopa (*L*-dopa, 100 mg/kg, ig) plus carbidopa (10 mg/kg, ig). Neurologic deficits were assessed, and the rats were sacrificed at 24 h after cerebral I/R surgery to measure brain infarct sizes. We conducted a proteomic analysis of the lesion side striatum samples and found that tyrosine metabolism and dopaminergic synapse were involved in the occurrence of cerebral stroke and the therapeutic effect of GSH. Western blot assay revealed that tyrosine hydroxylase (TH) mediated the occurrence of I/R-induced ischemic stroke and the therapeutic effect of GSH. We analyzed the regulation of GSH on endogenous small molecule metabolites and showed that exogenous GSH had the most significant effect on intrastriatal dopamine (DA) in I/R model rats by promoting its synthesis and inhibiting its degradation. To further explore whether DA-related alterations were potential targets of GSH, we investigated the therapeutic effect of DA accumulation on ischemic brain injury. The combined administration of the precursor drugs of DA (*L*-dopa and carbidopa) significantly ameliorated neurological deficits, reduced infarct size, and oxidative stress, and decreased pro-inflammatory cytokines levels in the striatum of I/R injury rats. More interestingly, exogenous *L*-dopa/carbidopa could also greatly enhance the exposure of intracerebral GSH by upregulating GSH synthetases and enhancing homocysteine (HCY) levels in the striatum. Thus, administration of exogenous GSH exerts a therapeutic effect on ischemic stroke by increasing intrastriatal DA, and the accumulated DA can, in turn, enhance the exposure of GSH and its related substances, thus promoting the therapeutic effect of GSH.

Keywords: glutathione; ischemia reperfusion; proteomics; tyrosine metabolism; dopamine

Acta Pharmacologica Sinica (2022) 43:541–551; https://doi.org/10.1038/s41401-021-00650-3

INTRODUCTION

Stroke remains the leading cause of death and permanent disability worldwide. Ischemic stroke, which is characterized by cerebral ischemia and neurological deficits, accounts for over 80% of the total incidence rate of stroke [1, 2]. Despite decades of research, there are still only two therapeutic methods in the clinic, including tissue plasminogen activators and endovascular devices [3]. In addition, only 3%–5% of stroke patients are able to benefit from these interventions due to potential contraindications and limited therapeutic time windows [4, 5]. Instroke patients, the loss of cerebral blood flow causes a decrease in oxygen content and an energy crisis in the ischemic region that leads to cerebral ischemia/reperfusion (I/R) brain injury [6, 7]. This highlights the need to gain a broader understanding of the mechanism of tissue damage and to search for effective drugs to improve the cure rate of ischemic stroke.

Gene expression studies have indicated that in the ischemic brain, the increased production of reactive oxygen species (ROS), highly active molecules that combine with cellular biomolecules, activates the gene expression of some neurodegenerative factors, such as apoptosis signals and pro-inflammatory cytokines, thus exacerbating ischemic injury [8]. Glutathione (GSH), an intracellular antioxidant tripeptide (c-*L*-glutamyl-*L*-cysteinyl-glycine), is the dominant nonprotein mercaptan in mammalian cells that, either alone or in concert with enzymes, reduces superoxide radicals, hydroxyl radicals, and peroxynitrites [9]. After GSH depletion, ROS accumulation and Ca^{2+} influx lead to programmed cell death, which is different from apoptosis [10]. The homogeneous balance of GSH at the optimal concentration and the ratio between reduction and oxidation in cells can be considered the basis of redox reactions in healthy cells [11]. In addition, the regulatory effects of GSH on two aspects of endothelial function are crucial for barrier protection: GSH protects endothelial cells from oxidative injury and controls cell proliferation during endothelial repair and/or wound healing [12]. Clinical studies have also shown that the GSH level is lower in the tissues of high-stroke-risk

[1]Key Lab of Drug Metabolism and Pharmacokinetics, State Key Laboratory of Natural Medicines, China Pharmaceutical University, Nanjing 210009, China and [2]College of Pharmacy, Nanjing University of Chinese Medicine, Nanjing 210046, China
Correspondence: Guang-ji Wang (guangjiwang@hotmail.com) or Yan Liang (liangyan0679@163.com)
These authors contributed equally: He Wang, Yi-sha Du, Wen-shuo Xu

Received: 7 December 2020 Accepted: 12 March 2021
Published online: 25 May 2021

individuals, and the GSH/GSSG ratio is also significantly reduced [13]. Administration of GSH-ethyl ester via the jugular vein at the onset of reperfusion in I/R model rats reduced infarct size and improved neurological outcome. The neuroprotective effect of GSH might be related to the increase in mitochondrial respiration and C-I activity [2]. Thus, GSH exerts ischemic neuronal protection through multiple targets and pathways.

DA, the precursor of the catecholamines noradrenaline and adrenaline, is considered a neurotransmitter and a signaling molecule, is produced by paraganglia, and plays crucial roles in a wide range of brain sensorimotor functions [14, 15]. There has been considerable interest in the potential role of DA in the central nervous system (CNS) ischemia and trauma. Several studies have suggested that the level of cerebral DA activity can also be significantly affected by other serious neurological diseases, especially stroke, but this has not been fully appreciated in basic research and clinical studies [16]. In the past few years, DA enhancers have been used to promote recovery from stroke. There has been strong evidence that DA enhancers can improve the motor recovery of stroke animal models through a series of potential mechanisms that are not yet fully understood [17, 18]. However, the interaction between stroke and the dopaminergic system is very complex, and understanding these interactions could lay the foundation for a better understanding of the effect of dopaminergic therapy after stroke.

In our previous study, we found that I/R surgery in rats greatly reduced the levels of GSH and cysteine (CYS) in the striatum and cortex of the damaged hemisphere, while oral administration of exogenous GSH significantly increased intracerebral GSH and CYS levels [19]. GSH was also proven to ameliorate the neurologic deficit score, infarct size, histologic lesions, pro-inflammatory cytokines, and blood-brain barrier (BBB) disruption in I/R model rats, but the underlying causes of these effects remain elusive. Because it has been suggested in the literature that DA can protect nerve cells from oxidative stress [17, 20], we wondered whether DA is involved in the treatment of brain injury by GSH. In the current study, we investigated the pathways of GSH based on a quantitative proteomic approach. Tyrosine metabolism and dopaminergic synapses were found to be involved in the occurrence of cerebral stroke and the treatment of GSH. In addition, exogenous GSH was found to significantly increase DA levels in the rat striatum by promoting DA synthesis and inhibiting DA degradation. Then, we focused on the interactions between GSH and DA in the treatment of ischemic stroke. The results demonstrated that the accumulation of intrastriatal DA also exerted a therapeutic effect against ischemic stroke. More interestingly, increased DA levels further increased the level of GSH in the striatum, thus improving the therapeutic effect of GSH.

MATERIALS AND METHODS

Materials

GSH (Lot No. B141015) was kindly supplied by Kunming Jida Pharmaceutical Co., Ltd. (Kunming, Yunnan, China). CYS, CYS-GLY, Glu, GLY, captopril (CAP), 2,7-dichlorofluorescein diacetate (DCFH-DA), iodoacetamide (IAM), dithiothreitol (DTT), and N-ethylmaleimide (NEM) were purchased from Sigma-Aldrich (St. Louis, MO, USA). Buthioninesulfoximine (BSO) was purchased from Aladdin (Shanghai, China). The assay kits for the measurement of interleukin-6 (IL-6), tumor necrosis factor-alpha (TNF-α), and interleukin-1β (IL-1β) were purchased from Shanghai Excell Biological Technology Co., Ltd. (Shanghai, China). Malondialdehyde (MDA), DCFH-DA, and Pierce™ BCA Protein Assay kits were purchased from Beyotime Biotechnology Co., Ltd. (Shanghai, China).

Animals and treatments

Animals. Male Wistar rats (220~240 g) were purchased from the Sipper-BK Laboratory Animal Co., Ltd. (Shanghai, China). The rats were randomly divided into different groups. They were housed under controlled conditions (25 °C, 55–60% humidity and a 12-h light/dark cycle) with free access to laboratory food and water. All studies were conducted in strict accordance with animal care regulations and guidelines and were approved by the Animal Care and Use Committee of China Pharmaceutical University.

Preparation of cerebral I/R model rats. For cerebral I/R model preparation, male Wistar rats were anesthetized by intraperitoneal injection of 10% chloral hydrate (0.3 mL/100 g) and subjected to focal cerebral ischemia. Briefly, the left common carotid artery, internal carotid artery, and external carotid artery were exposed through a midline incision in the neck. A silicone rubber-coated filament (0.28 mm in external diameter) was inserted into the internal carotid artery ~16–18 mm through the external carotid artery stump until the filament occluded the left middle cerebral artery. After middle cerebral artery occlusion (MCAO) for 2 h, the occluding filament was withdrawn to restore blood flow (reperfusion was confirmed by laser Doppler). In the sham-operated group, the blood vessels were exposed without blocking the middle cerebral artery. In the GSH-treated group, rats were intragastrically administered GSH at a dose of 250 mg/kg. Rats in the *L*-dopa/carbidopa-treated group were intragastrically administered 100 mg/kg *L*-dopa and 10 mg/kg carbidopa.

Neurologic assessment and measurement of infarct sizes. The neurologic assessment was performed by behavioral tests as previously described with minor modifications [21]. The modified scoring system was divided into five grades (0–4), and the scoring criteria were as follows: 0 points, normal walking, and no neurological deficits; 1 point, unable to fully extend the right forepaw; 2 points, unable to walk straight, circling to the right; 3 points, unable to walk normally, toppling to the right; and 4 points, unable to walk spontaneously and exhibiting depressed levels of consciousness. In addition, the rats were sacrificed at 24 h after cerebral I/R surgery to measure the infarct sizes of the rat brain. The collected brains were sectioned into consecutive 2 mm thick coronal slices using a cryomicrotome (Leica CM1950, Nussloch, Germany) and then immersed in 1% 2,3,5-triphenyl tetrazolium chloride (TTC) medium for 10 min at 37 °C. ImageJ 1.8.0 software was used to calculate infarct sizes.

Immunofluorescence staining of microglia in rat brain. Immunohistochemical analysis of rat brain: male Wistar rats were anesthetized with pentobarbital (50 mg/kg) and perfused with 20 mL of saline through the heart to remove blood cells. The tissues were fixed with 50 mL of buffered paraformaldehyde (4%; pH 7.2; 4–6 °C). The brains were immediately dissected and submerged in 20% sucrose in PBS (24 h, 4 °C) until completely saturated. Then, the brains were frozen at −80 °C and sliced into 50 μm thick sections. The brain sections were incubated with anti-IBA antibody (1:500) at 4 °C overnight, washed with PBS three times, and then incubated with green fluorescent-labeled secondary antibody for 1 h at room temperature. After washing with PBS three times, the images were collected under an inverted fluorescence microscope. ImageJ was used to calculate the perimeter and area of each microglia in the visual field. The ratio of perimeter to the area was calculated to evaluate the inflammatory injury caused by I/R surgery and the protective effects of GSH and DA on microglia.

Measurement of pro-inflammatory cytokines in rat brain. To evaluate the inflammatory injury caused by I/R surgery and the protective effects of GSH and DA, the levels of intracerebral IL-6, TNF-α, and IL-1β in the sham-operated, I/R model, I/R + GSH and I/R + DA groups were determined using the corresponding commercial ELISA kits (Excell Biological Technology) strictly

following the manufacturer's instructions. The contents of pro-inflammatory cytokines were calibrated by protein concentration.

Measurement of MDA level in rat brain. The rats were sacrificed at 24 h after cerebral I/R surgery, and brain tissue was collected. All brain specimens in the sham-operated, I/R model, I/R + GSH, and I/R + DA groups were processed according to the instructions of the Beyotime kit. The determination steps were carried out in strict accordance with the instructions. Finally, the OD values were detected by a microplate reader. The MDA and SOD levels were calculated by using standard curves.

Measurement of ROS level in rat brain. Oxidative stress levels were measured using a DCFH-DA staining assay. The rats were sacrificed at 24 h after cerebral I/R surgery, and the brain tissue was collected and weighed. Brain homogenate was prepared by adding PBS at a ratio of 1:10 (*w/v*). After centrifugation at 7104 × *g* for 10 min, 90 μL of supernatant was obtained. Then, 10 μM DCFH-DA was added to the supernatant and incubated in the dark at 37 °C for 30 min. The fluorescence intensity was read using a multifunctional fluorescent enzyme reader at an excitation wavelength of 488 nm and an emission wavelength of 525 nm.

Proteomics analysis. The rat ischemic hemisphere brain samples were processed for LTQ-Orbitrap XL MS analysis as we described previously [22]. Proteins in rat brains were denatured, alkylated, and trypsin-digested. The peptides were subsequently analyzed on the Thermo Fisher Ultimate 3000 RSLC Nano LC system and Thermo LTQ-Orbitrap XL MS. Chromatographic separation was performed on an Acclaim PepMap100 C18 reversed-phase trap column (75 μm × 2 cm, 3 μm, 100 Å, Thermo Fisher Scientific, USA). The LTQ-Orbitrap XL MS was operated in positive data-dependent acquisition mode to switch between MS [1] and MS/MS automatically. MS [1] survey scans (*m/z* 350-1800) were performed with a resolution of 60,000 at *m/z* 400. The ion spray voltage was 4500 V. The air curtain gas was 10 Arb, and the auxiliary gas was set at 50 psi. Protein discoverer software version 1.4 was used for the qualitative analysis of proteomics results. Proteins with an absolute fold change of <0.66 or >1.5 and a *P*-value < 0.05 were defined as DEPs. The gene ontology of DEPs was analyzed by Omics Bean. In addition, bioinformatics was used to study the biological process, cell composition, molecular function, and Kyoto encyclopedia of genes and genomes (KEGG) pathways.

Quantitative analysis of GSH, CYS, and CYS-GLY in the rat striatum. In our previous study, we established an LC-MS/MS method for the quantitative analysis of GSH, CYS, and CYS-GLY in a biological matrix [19]. Briefly, 100 μL of buffer solution containing 6 mg/mL Tris, 0.2 mg/mL serine, 1.24 mg/mL boric acid, 4 μg/mL acivicin and 7.76 mg/mL NEM was added to 10 mg of fresh rat striatum to prepare striatal homogenate. After derivatization for 1 h in a light-proof environment, 20 μL of internal standard solution (5 μg/mL captopril derivatized by NEM) was added to the tissue homogenate. Then, 200 μL of methanol was added to precipitate the proteins, and 5 μL of supernatant was analyzed using an LC-MS/MS system (SCIEX, MA, USA). Chromatographic separation was performed on a Sepax Bio-ODS SP column (4.6 mm × 150 mm, 5 μm). The optimized multiple reaction monitoring (MRM) parameters for GSH-NEM, CYS-NEM, CYS-GLY-NEM, and CAP-NEM were 433.1 → 304.1, 246.9 → 158.2, 304 → 287.1, and 343.1 → 228.1, respectively.

Quantitative analysis of neurotransmitters and amino acids. Ascorbic acid (20 mM) was added to 30 mg of the rat striatum. The mixtures were homogenized and sonicated in an ice bath. Then, 500 μL of ice-cold acetonitrile containing 200 ng of 2,5-dihydroxy benzoic acid was added to the homogenate. After drying under vacuum, 50 μL of borate buffer and 50 μL of benzoyl chloride were added for derivatization. The chromatographic separation was performed on an XBridge® Amide column (3.5 μm × 4.6 mm × 100 mm, Waters). The mobile phase consisted of solvent A (0.2% formic acid and 5.0 mM ammonium formate in water) and solvent B (acetonitrile). The MS was operated in the positive mode. Table S1 summarizes the MRM monitoring conditions for each analyte.

Quantitative analysis of GCLc, DRD4, and MS. TRIzol (1 mL, Invitrogen Co., San Diego, CA, USA) was added to 30 mg of rat striatum from the lesion side to prepare homogenate. Trichloromethane (200 μL) was added to the supernatant and shaken well. After standing for 5 min and centrifugation at 12,000 × *g* for 15 min at 4 °C, the upper layer was removed into a new EP tube, and 500 μL of isopropanol was added to precipitate RNA. Then, 1 mL of 75% ethanol was added to the RNA precipitated, washed, and centrifuged at 4 °C and 12000 × *g* for 5 min. The RNA precipitate was dried and dissolved in 10 μL of DEPC water. A Synergy H1 microplate reader of a multiwavelength measurement system (BioTek Instruments, Inc., Winooski, VT, USA) was used to quantify the RNA concentration and quality, and cDNA was synthesized using a High-Capacity RNA-to-cDNA Kit (Applied Biosystems, Foster City, CA, USA). Quantitative RT-PCR was performed on a Thermal Cycler Dice TM Real-Time System (TaKaRa Code: TP800). The primer sets for the target genes are listed in Table S1. Amplification was performed as follows: 5 min at 95 °C for template denaturation followed by 30 cycles at 60 °C for 15 s and 72 °C for 30 s.

Western blot analysis of tyrosine hydroxylase (TH). For Western blot analysis, the rat striatum was prepared as we previously described [23]. Briefly, rat striatum was isolated and homogenized in ice-cold lysis buffer. Protein concentrations in striatum homogenates were measured using a Thermo Scientific Pierce BCA Protein Assay Kit. The samples were diluted using Laemmli buffer and then denatured by heating to 95 °C for 5 min. The wells of a 10% acrylamide-bisacrylamide gel were loaded with 50 mg of protein. The voltage of the electrophoresis was set at 60 V and then increased to 90 V when the protein sample entered the separation gel. The proteins were subsequently transferred onto a polyvinylidene difluoride membrane and blocked in 5% non-fat milk with 0.1% Tween-20 in Tris buffer for 1 h followed by incubation overnight in the primary antibodies at 4 °C. The membrane was then washed three times and incubated with the appropriate secondary antibodies. Bound immunoglobulins were visualized with the Super Signal West Pico Chemiluminescent Substrate (Pierce/Thermo Fisher Scientific) on a G:BOX chemiXR5 system. The grayscale analysis was carried out using ImageJ software (National Institutes of Health, Open Source).

RESULTS

Proteomic investigation of the mechanism of I/R-induced ischemic stroke and the therapeutic effect of GSH

The whole proteome in lesion-side striatum tissue from sham-operated, I/R model and I/R + GSH rats were analyzed by LTQ-Orbitrap XL MS to preliminarily investigate the molecular mechanism and potential targets of GSH. Label-free analysis of the identified proteins from the three groups was then conducted by Max Quant software, and the proteomic data were analyzed by PCA. As shown in Fig. 1a, there was a significant difference in the proteome between the sham group and the I/R group. After exogenous GSH was administered, the proteome of the I/R + GSH group was similar to that of the sham group, which further proved the therapeutic effect of GSH on ischemic stroke. We then identified the differentially expressed proteins between the sham-operated group and the I/R group by identifying genes that were upregulated at least 1.5-fold or down-regulated at least 0.66-fold with a *P* value of less than 0.05. As shown in Fig. 1b, the expression

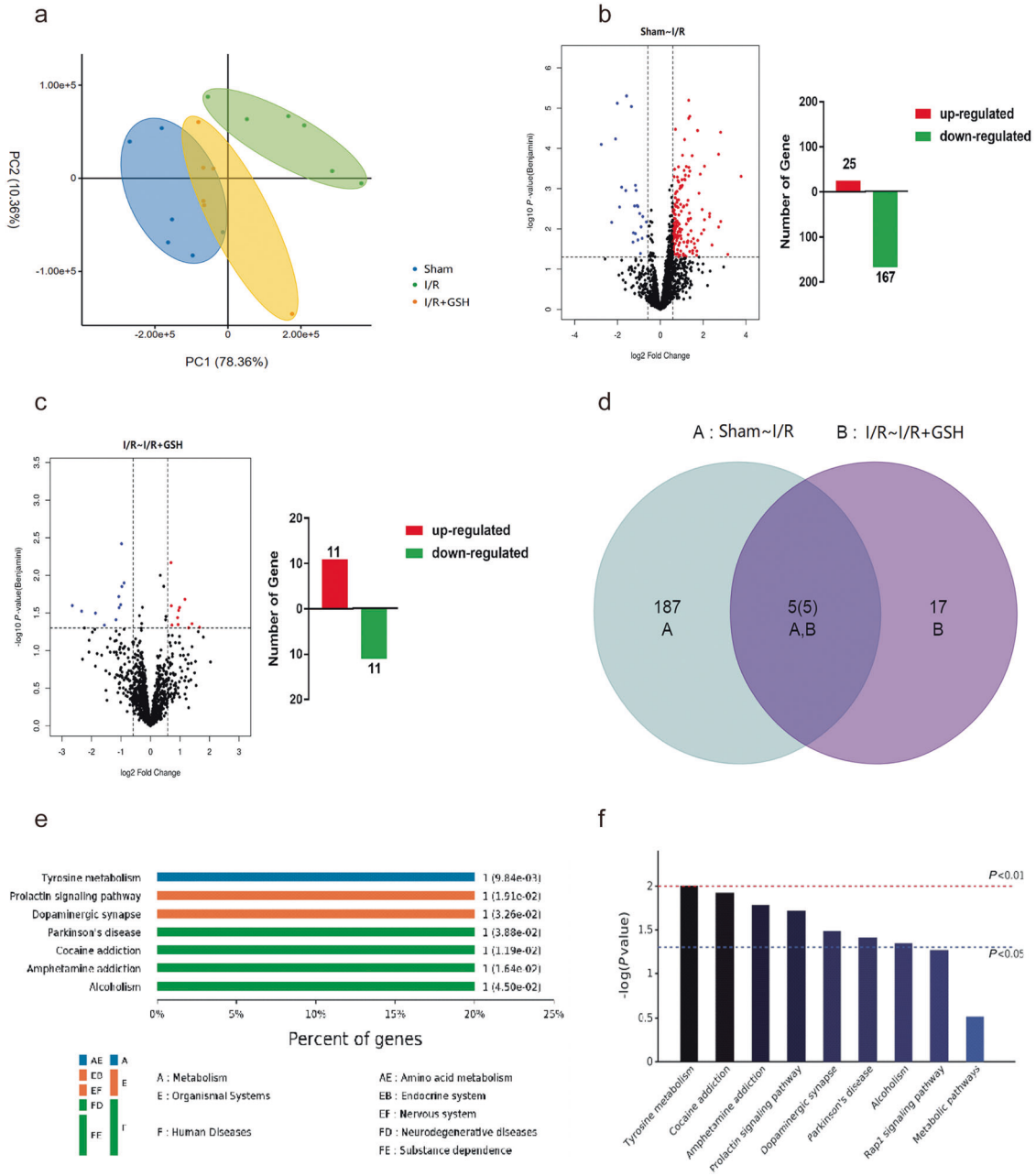

Fig. 1 Proteomic investigation of the mechanism of I/R-induced ischemic stroke and the therapeutic effect of GSH. a Principal component analysis of cerebral proteome in sham-operated group, I/R group, and I/R + GSH group. **b** Volcanic map and the number of regulatory proteins of differentially abundant proteins in the brains of the sham-operated group and the I/R group. **c** Volcanic map and the number of regulatory proteins of differentially abundant proteins in the focal brains of the I/R group and I/R + GSH group. **d** Venn diagram of differentially abundant proteins in the focal brains of the sham-operated group, the I/R group, and I/R + GSH group. **e** Grading of enriched KEGG pathway in sham-operated group, I/R group, and I/R + GSH group. **f** KEGG pathway of significantly differential proteins in sham-operated group, I/R group, and I/R + GSH group.

levels of 192 DEPs (Group A) were significantly changed after cerebral I/R; among them, 167 DEPs were downregulated and 25 DEPs were significantly upregulated. In addition, 22 DEPs (Group B) were identified between the I/R and I/R + GSH groups, among which 11 DEPs were upregulated and the other 11 were downregulated (Fig. 1c). Furthermore, Venn diagram analysis revealed that 5 DEPs were identified in both Group A and Group B (Fig. 1d), which suggests that GSH administration may exert pharmacological effects on cerebral I/R injury through these 5 DEPs. KEGG was used to analyze the signal transduction pathway and biochemical metabolic pathway, and the enriched KEGG pathway, and the results showed that these common DEPs were involved in tyrosine metabolism ($P = 9.84 \times 10^{-3}$), the prolactin signaling pathway ($P = 1.19 \times 10^{-2}$), and dopaminergic synapses ($P = 3.26 \times 10^{-2}$) (Fig. 1e). It is clear that modulation of these signaling pathways, including tyrosine metabolism and dopaminergic synapses, is the main cause of I/R development and underlies the therapeutic effect of GSH (Fig. 1f).

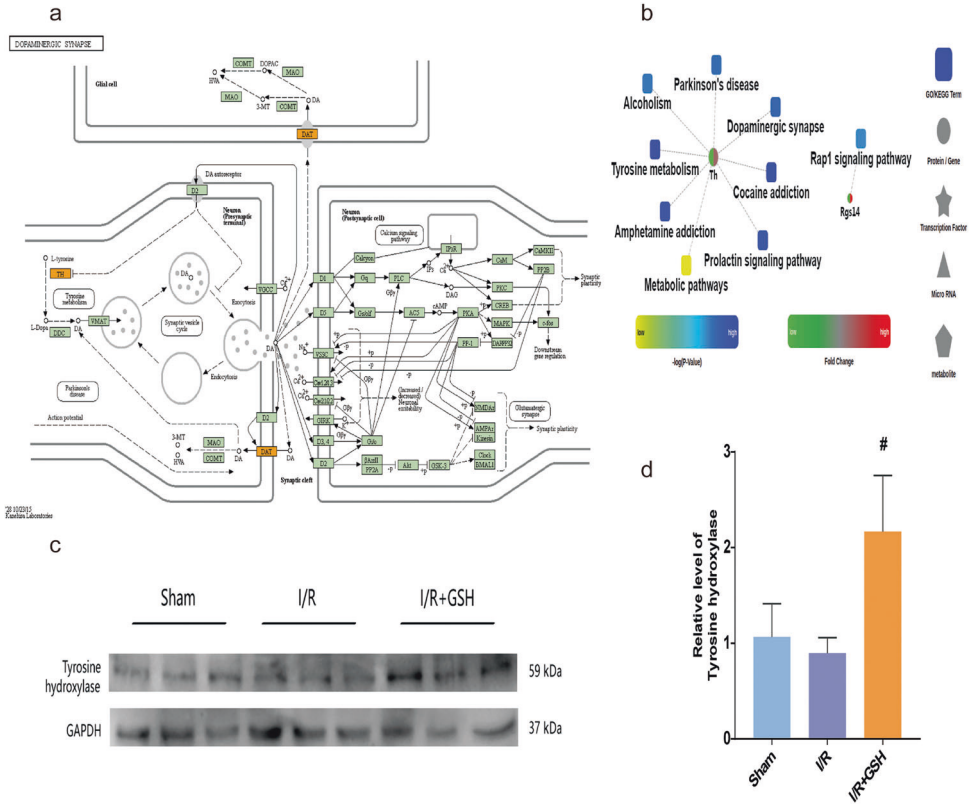

Fig. 2 Effect of I/R operation and GSH on the expression of tyrosine hydroxylase. a KEGG pathway of the dopaminergic synapse. **b** Protein–protein interaction diagram. **c**, **d** Western blot analysis and relative quantification of TH in the striatum of rats in sham-operated group, I/R group, and I/R + GSH group. Data were expressed as mean ± SD. *$P < 0.05$, **$P < 0.01$, ***$P < 0.001$, ****$P < 0.0001$.

Effect of I/R operation and GSH on the expression of TH

DA is a crucial neurotransmitter that stimulates the brain and its reward center. Tyrosine is the precursor of DA. After GSH treatment, the signaling pathways disrupted by I/R surgery, including tyrosine metabolism and dopaminergic synapses, were restored to normal levels. Furthermore, analysis of common DEPs in the dopaminergic neuron pathway showed that the I/R operation significantly downregulated the regulatory proteins TH and DA transporter, and GSH greatly reversed this downregulation (Fig. 2a). A proteomic network involving the dysregulated DEPs was constructed to visualize the protein–protein interactions. Clearly, the TH protein was significantly downregulated after cerebral I/R injury (Fig. 2b). GSH administration significantly reversed the downregulation of TH, suggesting that DA may mediate the therapeutic effect of GSH. In addition, GSH significantly reduced the protein expression of Rgs14 after cerebral I/R injury, suggesting that GSH plays an important role in synaptic signal transduction, learning, and memory integration. Then, the protein expression of TH in the sham operation, I/R model, and I/R + GSH rats was measured by Western blotting to further verify the reliability of the proteomic results. Clearly, I/R surgery caused the downregulation of the TH enzyme, and exogenous GSH significantly enhanced the expression of TH (Fig. 2c, d). Therefore, the results of the Western blot assay were consistent with those of the proteomic analysis. TH mediated the occurrence of I/R-induced ischemic stroke and the therapeutic effect of GSH.

Effects of I/R operation and exogenous GSH on intracerebral DA levels

The proteomic analysis revealed that the mechanism of GSH in ischemic brain injury might be related to tyrosine metabolism and dopaminergic synapses. Thus, the mechanism was further explored by investigating the effects of I/R surgery and GSH treatment on NTs and AAs. The striatum of sham-operated, I/R model and GSH-treated rats was analyzed by LC-MS/MS to detect 24 NTs and AAs, including tyrosine (Tyr), phenylalanine (Phe), DA, Gly, glutamine (Gln), serotonin (5-HT), γ-aminobutyric acid (GABA), choline (CH), serine (Ser), alanine (Ala), Glu, tryptophan (Trp), leucine (Leu), asparagine (Asn), threonine (Thr), arginine (Arg), valine (Val), proline(Pro), lysine (Lys), 3-hydroxyanthranilic acid (3-HAA), 3,4-dihydroxyphenylacetic acid (DOPAC), homovanillic acid (HVA), 5-hydroxyindole-3-acetic acid (5-HIAA), and methionine (Met). As shown in Fig. 3a, the levels of DA, GABA, 5-HT, Tyr, Gly, and Gln in the I/R group were significantly lower than those in the sham operation group, and exogenous administration of GSH greatly increased the levels of DA and Gly in I/R rats. In addition, the levels of HVA, Ala, Glu, Lys, Trp, Val, Pro, Ser, and Arg were significantly increased by the I/R operation, and GSH administration significantly reversed the increases in HVA, Ala, Glu, Trp, and Val in I/R rats. Notably, I/R operation and GSH administration had the most significant effects on DA levels.

To further confirm the changes in DA and its metabolites, the concentrations of DA, DOPAC, and HVA in the striatum of the sham, I/R, and I/R + GSH groups were statistically analyzed. Clearly, the level of DA in the striatum of I/R rats was significantly lower than that of sham-operated rats (one-way ANOVA, $P < 0.0001$), and exogenous GSH restored the level of DA in the striatum of I/R rats to a normal level (Fig. 3b). More interestingly, DOPAC and HVA showed the opposite changes from DA (Fig. 3c, d). To explore the mechanism of the effects of I/R surgery and exogenous GSH on the regulation of intracerebral DA, we used ELISA kits to detect the expression of enzymes related to DA synthesis and metabolism. The results showed that exogenous GSH significantly upregulated the protein expression of TH and DA decarboxylase (DDC) in the rat striatum (Fig. 3e, f). Moreover, the high expression

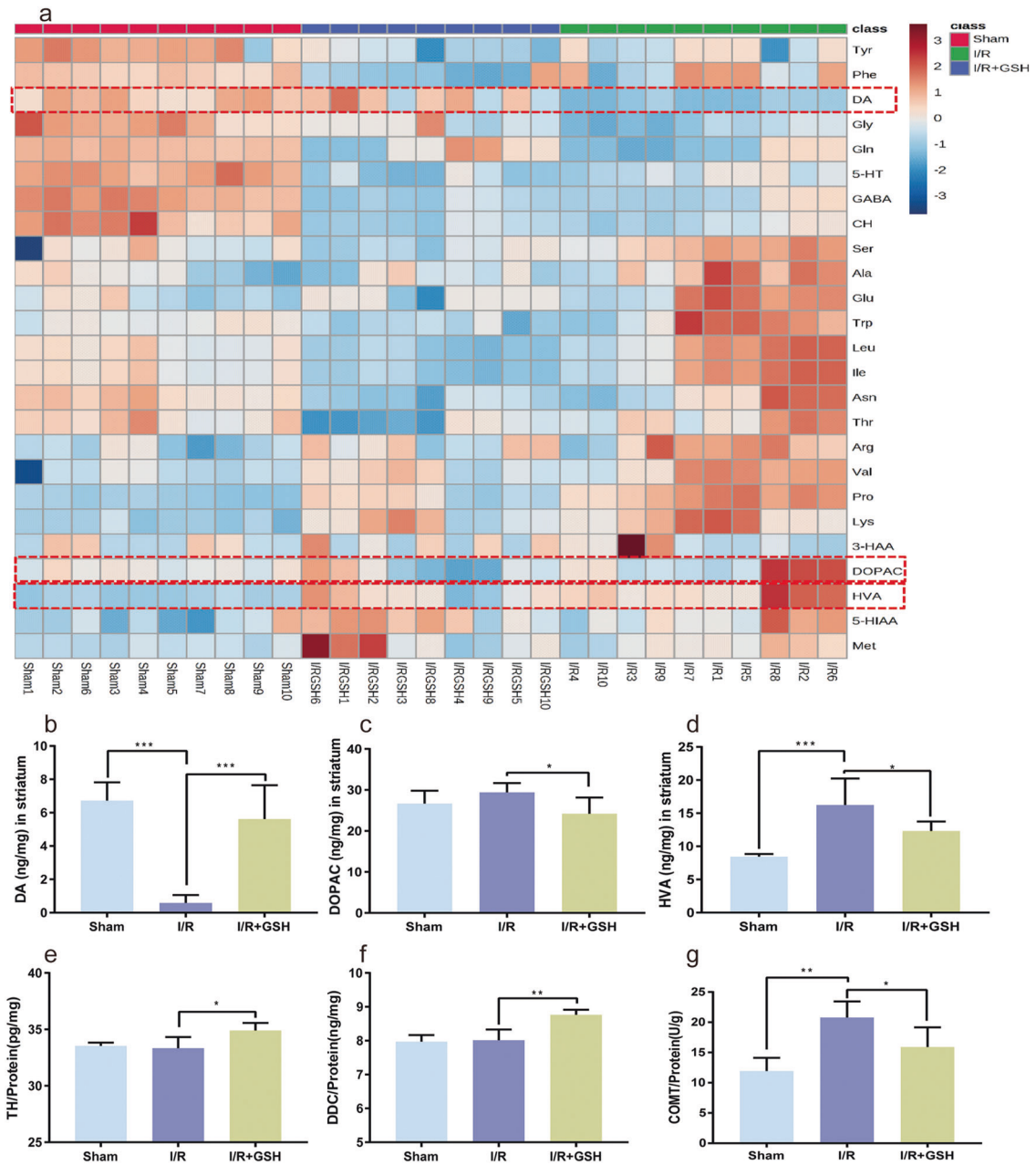

Fig. 3 Effects of I/R operation and exogenous GSH on intracerebral DA levels. a Quantitative analysis of neurotransmitters and amino acids. **b**–**d** Levels of DA (**b**), DOPAC (**c**), and HVA (**d**) in the striatum of the focal side in sham-operated group, I/R group, and I/R + GSH group. **e**–**g** Levels of TH (**e**), DDC (**f**), and COMT (**g**) in the striatum of rats.

of catechol-O-methyl transferase (COMT) caused by I/R was reversed by GSH administration (Fig. 3g). Therefore, GSH treatment increased the level of DA in the striatum by promoting the synthesis and inhibiting the degradation of DA.

Investigation of the therapeutic effect of oral DA on I/R-induced ischemic stroke

Combined administration of *L*-dopa (100 mg/kg) and carbidopa (10 mg/kg) was used to study the physiological significance of DA accumulation in the striatum. The rats were divided into sham operation, I/R model, I/R + GSH, and I/R + *L*-dopa/carbidopa groups. Brain infarct volume was estimated using a TTC staining assay. As shown in Fig. 4a, cerebral infarction was obvious after I/R surgery. The degree of ischemia in the *L*-dopa/carbidopa- and GSH-treated groups was significantly lower than that in the I/R model group. Oral administration of *L*-dopa/carbidopa and GSH reduced the infarct size from 27.62% to 4.98% and 5.43%, respectively (Fig. 4b). Furthermore, both *L*-dopa/carbidopa and GSH greatly decreased the neurological deficit score of I/R model rats (Fig. 4c). Then, the levels of intracerebral pro-inflammatory cytokines (TNF-α, IL-1β, and IL-6) were determined to further investigate the therapeutic effect of DA on I/R injury. As shown in Fig. 4d, f, *L*-dopa/carbidopa, like GSH, significantly reversed the upregulation of pro-inflammatory cytokines induced by I/R surgery.

ROS are produced by cells in the process of metabolism. High concentrations of ROS induce the apoptosis and even necrosis of cells through oxidative stress. Next, the effect of DA on oxidative stress was investigated by labeling ROS in PC12 cells with a DCFH-DA fluorescent probe. As shown in Fig. 5a, b, hypoxia-reoxygenation

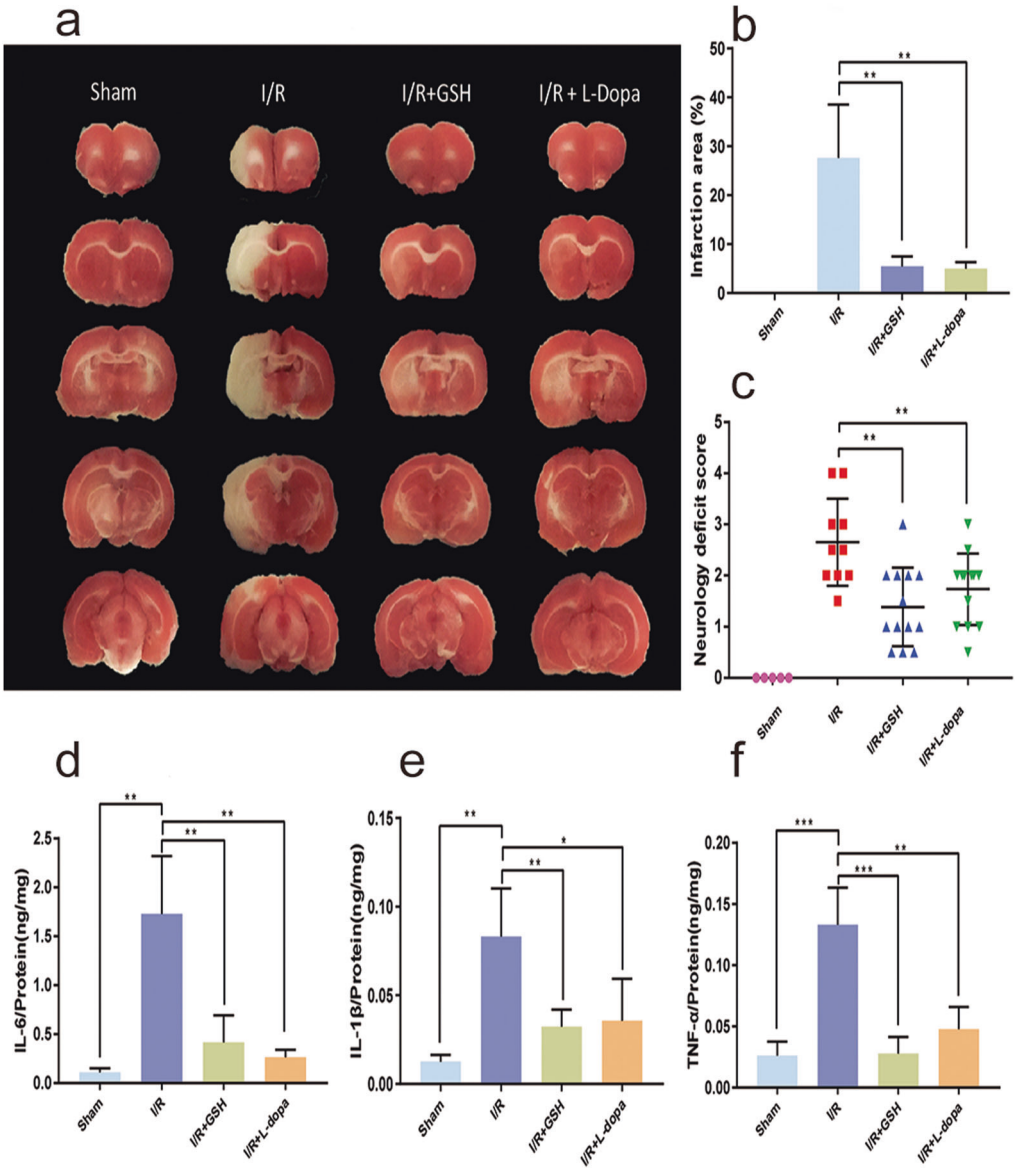

Fig. 4 The therapeutic effect of oral DA on I/R-induced ischemic stroke. a, **b** TTC staining (**a**) and percentage of cerebral infarction area (**b**) in sham-operated group, I/R group, I/R + GSH group, and I/R + *L*-dopa group. **c** Longa behavior scores of rats. **d**–**f** Levels of IL-6 (**d**), IL-1β (**e**), and TNF-α (**f**) in the brain of rats.

(OGD/R) significantly increased ROS levels in PC12 cells. After incubating PC12 cells with different concentrations of GSH (0.5, 5, and 20 μM), ROS decreased in a concentration-dependent manner. Similarly, exogenous DA (0.5, 5, and 20 μM) also reduced ROS levels in a dose-dependent manner. The activation of microglia is closely related to the severity of stroke. We then investigated the effects of GSH and DA on microglial activation after ischemic brain injury with an immunofluorescence assay. Compared with those in the control group, the microglia in the I/R model group were larger in volume, had fewer protrusions, and were more amoeboid in shape (Fig. 5c, d). After administration of GSH, the number of microglia in I/R model rats increased, and the cell bodies became smaller. There was no significant difference in the perimeter-to-area ratio between the I/R + GSH group and the sham operation group. In addition, the effect of DA on the volume and shape of microglia was similar to that of GSH, which suggested that both GSH and *L*-dopa/carbidopa can inhibit the activation of microglia. Therefore, exogenous GSH exerted a therapeutic effect on ischemic stroke by enhancing intrastriatal DA, thus reducing the levels of inflammatory factors, decreasing oxidative stress, and inhibiting the activation of microglia in I/R rats.

Effects of exogenous DA on the levels of GSH and related substances

GSH and DA are endogenous substances and mediate a variety of physiological and pathological processes. As GSH increased intrastriatal DA, we were interested in determining whether GSH could interact with DA in the treatment of stroke. Therefore, we next investigated the effects of exogenous DA on the levels of GSH and related substances. The results showed that *L*-dopa/carbidopa treatment significantly reversed the decrease in GSH concentration caused by the I/R operation (Fig. 6a). In addition, GSH administration increased the level of GSH to some extent, but the degree of increase was even lower than that induced by *L*-dopa/carbidopa. Exogenous GSH and *L*-dopa/carbidopa both significantly increased the level of intrastriatal CYS, and the increase induced by GSH was slightly higher than that of *L*-dopa/

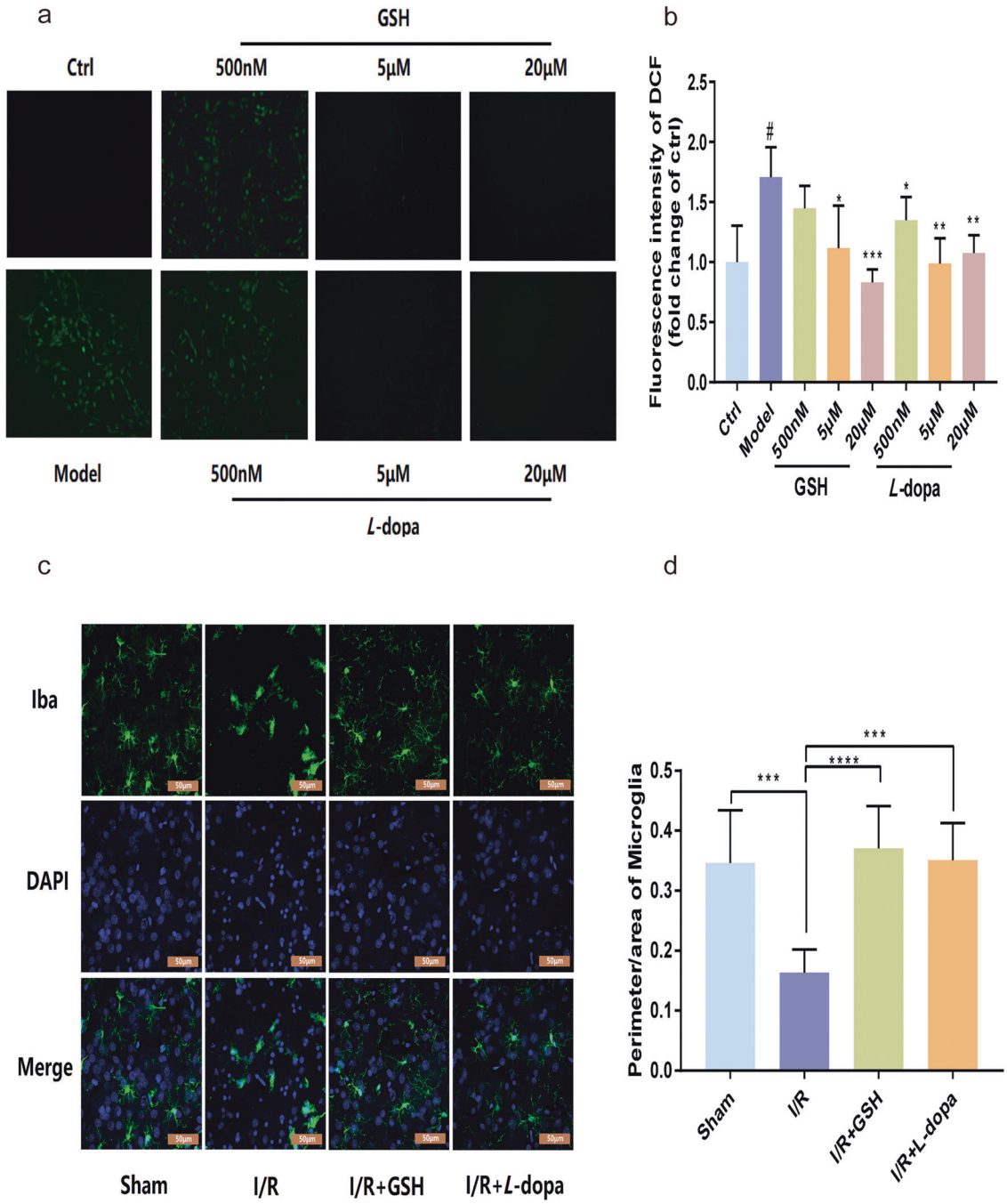

Fig. 5 The therapeutic effect of oral DA on I/R-induced ischemic stroke. a Fluorescence image of intracellular ROS in sham-operated group, I/R group, I/R + GSH group, and I/R + *L*-dopa group. **b** Fluorescence intensity of intracellular ROS. **c**, **d** Immunofluorescence imaging (**c**) of microglial and cell perimeter area ratio (**d**). Data were expressed as mean ± SD. **P* < 0.05, ***P* < 0.01, ****P* < 0.001, *****P* < 0.0001.

carbidopa(Fig. 6b). The level of Glu in the rat striatum was significantly higher than that of GSH or CYS. I/R surgery increased the level of Glu in the striatum to a certain extent, but the Glu levels in the sham, I/R model, I/R + GSH, and I/R + *L*-dopa/carbidopa groups were not significantly different (Fig. 6c). The level of GLY was also higher than that of GSH and CYS. I/R operation caused a decrease in GLY. Exogenous GSH increased the concentration of GLY, while *L*-dopa/carbidopa had no significant effect on intrastriatal GLY (Fig. 6d). The level of CYS-GLY in the rat striatum was extremely low (< 20 ng/g), and the I/R operation caused a further decrease in intrastriatal CYS-GLY. Exogenous GSH and *L*-dopa/carbidopa significantly increased the level of CYS-GLY in the striatum of I/R model rats (Fig. 6e). Therefore, the upregulation of intracerebral DA might further promote the therapeutic effects of GSH in I/R-induced ischemic stroke by increasing the levels of GSH, CYS, and CYS-GLY.

Mechanism of DA-mediated regulation of GSH-related substances

To reveal the mechanism by which DA upregulates GSH, we investigated the effects of DA on enzymes related to the GSH synthesis pathway. γ-Glutamylcysteine ligases (GCLs), including the catalytic subunit (GCLc) and the regulatory subunit (GCLm), are the rate-limiting enzymes involved in GSH synthesis in vivo. GCLc has all the catalytic activities of GCLs and performs the first

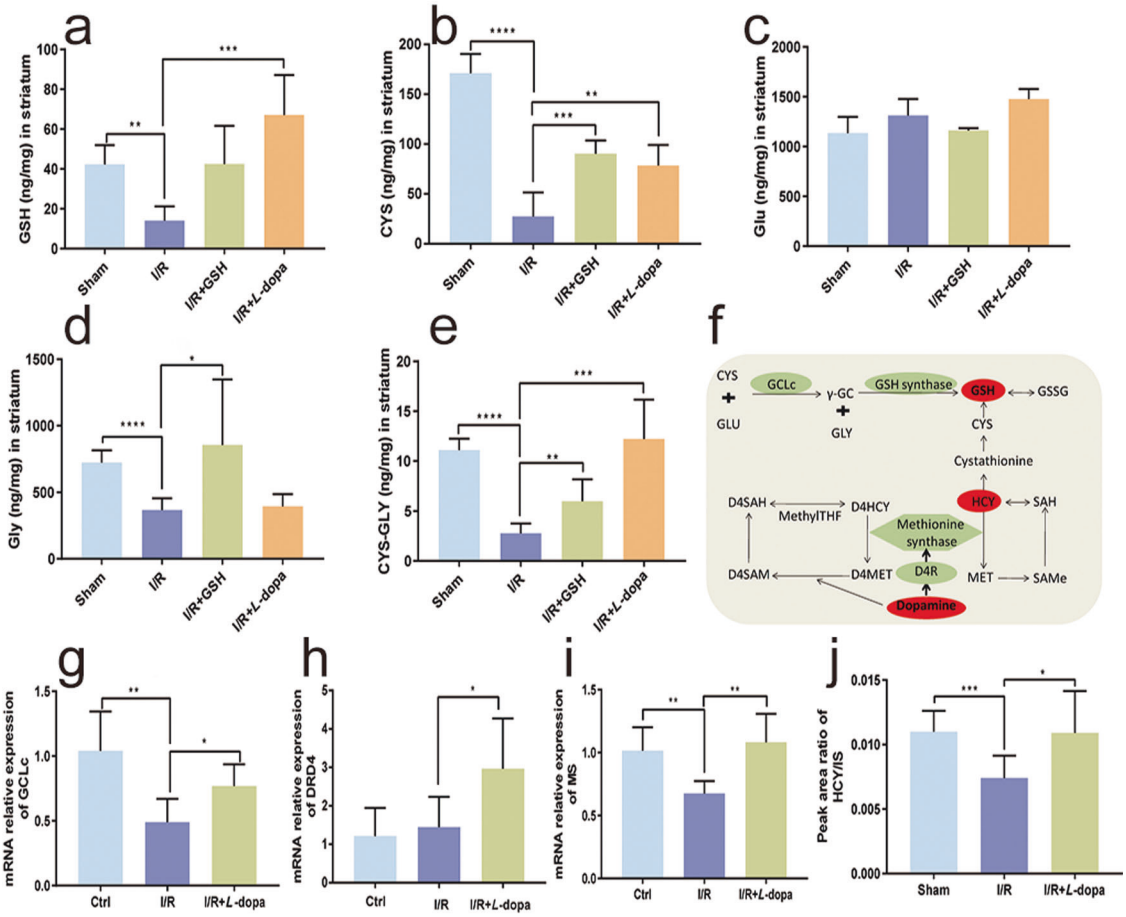

Fig. 6 Effects of exogenous DA on the levels of GSH and its related substances. Levels of GSH (**a**), Cys (**b**), Glu (**c**), Gly (**d**), and CYS-GLY (**e**) in the striatum of the focal side in the sham-operated group, I/R group, I/R + GSH group, and I/R + *L*-dopa group. **f** The synthesis and metabolism of GSH. **g**–**j** Levels of GCLc (**g**), DRD4 (**h**), MS (**i**), and HCY (**j**) in the brain of rats. Data were expressed as mean ± SD. $^{*}P < 0.05$, $^{**}P < 0.01$, $^{****}P < 0.0001$.

rate-limiting step in GSH synthesis [24]. In addition, the dopamine D4 receptor (DRD4), methionine synthase (MS), and homocysteine (HCY) also played important roles in the synthesis and metabolism of GSH (Fig. 6f). We then examined the influence of *L*-dopa/carbidopa administration on the expression of GCLc. As shown in Fig. 6g, GCLc expression in the rat striatum was significantly downregulated by the I/R operation. Oral administration of *L*-dopa/carbidopa significantly reversed the downregulation of GCLc expression caused by the I/R operation. The expression of DRD4 is closely related to the basic levels of methionine, S-adenosylmethionine, S-adenosyl homocysteine, CYS, and GSH [25]. Our results showed that I/R surgery had no obvious effect on the expression of DRD4, but exogenous *L*-dopa/carbidopa significantly increased the expression of DRD4 in the rat striatum (Fig. 6h). In addition, some studies have indicated that when oxidative stress occurs, MS activity is reduced, which causes more HCY to be converted to CYS via transsulfuration, thus augmenting the synthesis of the antioxidant GSH [24, 25]. As shown in Fig. 6i, I/R surgery significantly reduced the expression of MS in the rat striatum, and exogenous *L*-dopa/carbidopa significantly reversed the downregulation of MS expression caused by I/R. Since HCY plays a role in the synthesis of GSH, we then established a relative quantitative method for the determination of HCY levels in the rat striatum to investigate the effect of DA on HCY. The results demonstrated that the HCY level in the striatum of I/R model rats was significantly lower than that of sham-operated rats, and exogenous *L*-dopa/carbidopa increased the level of HCY in I/R model rats (Fig. 6j).

DISCUSSION

Ischemic stroke, a leading cause of long-term disability and mortality, causes a substantial burden on patients and communities worldwide [26]. The current FDA-approved stroke treatments are limited to intravenous administration of tissue plasminogen activator and intravascular thrombectomy. However, both therapies are limited by narrow treatment windows [27]. It is still the focus of clinicians and researchers to treat stroke and promote functional recovery after ischemic stroke. GSH, a key determinant of redox signaling, performs several vital functions, including maintenance of redox potential, antioxidant defense, regulation of cell cycle progression and apoptosis, detoxification of xenobiotics, modulation of immune function, and fibrogenesis [25]. Our previous studies showed that the oral administration of GSH not only had a direct therapeutic effect on cerebral stroke by stabilizing brain GSH, CYS, and Glu levels but also had an indirect therapeutic effect by increasing the intestinal levels of GSH, CYS, CYS-GLY, and γ-GC and reducing intestinal barrier damage. However, the underlying mechanism of GSH in the treatment of brain injury is still unclear, and further research is urgently needed to clarify potential targets.

To further clarify the underlying mechanism of GSH in the treatment of stroke, we first tried to identify the GSH pathway using proteomic analysis. The striatum plays a pivotal role in several neurodegenerative disorders and regulates motor behavior by receiving afferent inputs from the cerebral cortex and the ventromedial, ventrolateral, and mediodorsal thalamic nuclei [28]. In this study, the global proteome on the lesion-side of the

striatum in sham-operated, I/R model and I/R + GSH rats was compared, and all the DEPs underwent biological functional analysis. The results of the biological functional analysis showed that exogenous GSH mainly regulated proteins related to learning and memory, DA biosynthesis, neurotransmitter circulation, protein regulation and localization, and metabolic processes (Fig. S1a). These DEPs were involved in protein binding, catalytic reactions, oxygen reduction, signal transduction, and other processes (Fig. S1b). There were significant differences in DEPs related to synapses, extracellular vesicles, neural inputs, and transport vesicles, among which synapses and neurons accounted for the majority (Fig. S1c). KEGG was used to analyze the signal transduction pathway and biochemical metabolic pathway, and the results showed that the altered DEPs were strongly associated with the pathways related to tyrosine metabolism and DA synthesis. To further verify the reliability of the proteomics results, the protein expression of TH in lesion-side striatum of sham-operated, I/R model and I/R + GSH rats was measured by Western blot. The Western blot results were consistent with the proteomics results. The mechanism by which GSH reduces ischemic brain injury may be related to the regulation of DA.

DA, the most abundant neurotransmitter in the basal ganglia, is synthesized in the large-diameter neurons of the substantia nigra and released from the terminals that reside within the striatum [29]. Previous studies have shown that DA is involved in most brain functions during brain development and is associated with nervous system diseases such as PD, ischemic stroke, and others [30]. In the present study, the levels of DA and its metabolites (DOPAC and HVA) in rat striatum were quantitatively analyzed. The results showed that I/R operation not only reduced the DA level but also increased the concentration of HVA. Exogenous GSH restored DA and its metabolites to normal levels. To further investigate the mechanism of the effects of I/R surgery and exogenous GSH on intracerebral DA, we measured the expression of DA synthesis- and metabolism-related enzymes. Exogenous GSH was found to not only increase the expression of DA synthesis enzymes (TH and DDC) but also significantly downregulate the expression of COMT, an enzyme involved in DA metabolism.

To further investigate whether DA-related alterations were induced by GSH, we systematically studied the effect of accumulated DA on ischemic brain injury. As shown in Fig. S2a, the combination of *L*-dopa and carbidopa significantly increased the concentration of DA in the rat striatum. *L*-dopa/carbidopa administration also significantly reduced the infarct size, neurological deficit score, and level of pro-inflammatory cytokines (TNF-α, IL-1β, and IL-6) in the striatum. Ample evidence has indicated that after acute ischemic stroke, the rapid increase in ROS quickly overwhelms antioxidant defenses, which leads to autophagy, apoptosis, and necrosis [31]. In the present study, the effect of DA on oxidative stress was investigated by labeling ROS in PC12 cells and the rat striatum. In OGD/R-injured PC12 cells, DA reduced ROS levels in a dose-dependent manner. Both GSH and DA significantly reduced ROS levels in the striatum of I/R model rats (Fig. S2b). In addition, GSH also greatly reduced the level of MDA, but DA did not have a significant effect on the MDA level (Fig. S2c). Previous reports have revealed that microglial activation is closely related to the severity of stroke. We next compared the volume, protrusions, and shape of microglia prepared from sham-operated, I/R, I/R + GSH, and I/R + *L*-dopa/carbidopa rats. After the administration of GSH or *L*-dopa/carbidopa, the number of microglia increased markedly, and the cell volume decreased significantly, which suggested that both GSH and *L*-dopa inhibited the activation of microglia. Therefore, exogenous GSH decreased the levels of inflammatory factors, reduced oxidative stress, and inhibited the activation of microglia by increasing DA levels in the striatum, thus exerting a therapeutic role in ischemic stroke.

GSH and DA are both endogenous substances that participate in many biological phenomena and play important roles in nervous system diseases. Since GSH increased the level of intracerebral DA, we wondered whether GSH interacts with DA in the treatment of ischemic stroke. Then, the effects of exogenous DA on the global levels of GSH and related substances were investigated. GSH is a cysteine-containing tripeptide synthesized from CYS, and exogenous DA was found to cause a threefold increase in the CYS level. In addition, exogenous DA caused a fivefold increase in CYS-GLY but had no obvious effect on Glu or GLY. Then, the enzymes involved in GSH synthesis, including GCLc, DRD4, and MS, were measured to reveal the mechanism by which DA upregulates GSH-related substances in the rat striatum. We found that GCLc and MS expression in the rat striatum was significantly reduced by the I/R operation and oral administration of *L*-dopa/carbidopa significantly reversed the downregulation of GCLc and MS. In addition, HCY is a raw material used to generate CYS and GSH, and the HCY level in the rat striatum was quantified to investigate the effect of DA on HCY. The decreased intrastriatal HCY was restored by exogenous *L*-dopa/carbidopa.

ACKNOWLEDGEMENTS

This study was supported by Innovative Research Groups of the National Natural Science Foundation of China (Grant No. 81421005), Sanming Project of Medicine in Shenzhen (SZSM201801060), and the Natural Science Foundation of Hebei Province (Grant no. 2020208022 and 20208025).

AUTHOR CONTRIBUTIONS

YL, HW, YSD, and WSX designed the experiments. HW, YSD, WSX, CJL, HS, KRH, ZYH, TJY, and HMG performed the experiments and analyzed the data. YL, GJW, LX, HW, YSD, and WSX prepared the original manuscript.

ADDITIONAL INFORMATION

Supplementary information The online version contains supplementary material available at https://doi.org/10.1038/s41401-021-00650-3.

Competing interests: The authors declare no competing interests.

REFERENCES

1. Li X, Guo H, Zhao L, Wang B, Liu H, Yue L, et al. Adiponectin attenuates NADPH oxidase-mediated oxidative stress and neuronal damage induced by cerebral ischemia-reperfusion injury. Biochim Biophys Acta Mol Basis Dis. 2017;1863:3265–76.
2. Kahl A, Stepanova A, Konrad C, Anderson C, Manfredi G, Zhou P, et al. Critical role of flavin and glutathione in complex I-mediated bioenergetic failure in brain ischemia/reperfusion injury. Stroke. 2018;49:1223–31.
3. Campbell BC, Meretoja A, Donnan GA, Davis SM. Twenty-year history of the evolution of stroke thrombolysis with intravenous alteplase to reduce long-term disability. Stroke. 2015;46:2341–6.
4. Hacke W, Kaste M, Bluhmki E, Brozman M, Dávalos A, Guidetti D, et al. Thrombolysis with alteplase 3 to 4.5 h after acute ischemic stroke. N Engl J Med. 2008;359:1317–29.
5. Deb P, Sharma S, Hassan KM. Pathophysiologic mechanisms of acute ischemic stroke: an overview with emphasis on therapeutic significance beyond thrombolysis. Pathophysiology. 2010;17:197–218.
6. Donnan GA, Fisher M, Macleod M, Davis SM. Stroke. Lancet. 2008;371:1612–23.
7. Chen G, Ye X, Zhang J, Tang T, Li L, Lu P, et al. Limb remote ischemic postconditioning reduces ischemia-reperfusion injury by inhibiting NADPH oxidase activation and MyD88-TRAF6-P38MAP-kinase pathway of neutrophils. Int JMol Sci. 2016;17:1971.
8. Rodrigo R, Fernández-Gajardo R, Gutiérrez R, Matamala JM, Carrasco R, Miranda-Merchak A, et al. Oxidative stress and pathophysiology of ischemic stroke: novel therapeutic opportunities. CNS Neurol Disord Drug Targets. 2013;12:698–714.
9. Ammal Kaidery N, Thomas B. Current perspective of mitochondrial biology in Parkinson's disease. Neurochem Int. 2018;117:91–113.

10. Maher P, Schubert D. Signaling by reactive oxygen species in the nervous system. Cell Mol Life Sci. 2000;57:1287–305.
11. Ballatori N, Krance SM, Notenboom S, Shi S, Tieu K, Hammond CL. Glutathione dysregulation and the etiology and progression of human diseases. Biol Chem. 2009;390:191–214.
12. Li W, Busu C, Circu ML, Aw TY. Glutathione in cerebral microvascular endothelial biology and pathobiology: implications for brain homeostasis. Int J Cell Biol. 2012;2012:434971.
13. Namba K, Takeda Y, Sunami K, Hirakawa M. Temporal profiles of the levels of endogenous antioxidants after four-vessel occlusion in rats. J Neurosurg Anesthesiol. 2001;13:131–7.
14. Villanueva I, Piñón M, Quevedo-Corona L, Martínez-Olivares R, Racotta R. Epinephrine and dopamine colocalization with norepinephrine in various peripheral tissues: guanethidine effects. Life Sci. 2003;73:1645–53.
15. Pfeil U, Kuncova J, Brüggmann D, Paddenberg R, Rafiq A, Henrich M, et al. Intrinsic vascular dopamine - a key modulator of hypoxia-induced vasodilatation in splanchnic vessels. J Physiol. 2014;592:1745–56.
16. Momosaki S, Ito M, Yamato H, Iimori H, Sumiyoshi H, Morimoto K, et al. Longitudinal imaging of the availability of dopamine transporter and D2 receptor in rat striatum following mild ischemia. J Cereb Blood Flow Metab. 2017;37:605–13.
17. Ishige K, Chen Q, Sagara Y, Schubert D. The activation of dopamine D4 receptors inhibits oxidative stress-induced nerve cell death. J Neurosci. 2001;21:6069–76.
18. Gower A, Tiberi M. The intersection of central dopamine system and stroke: potential avenues aiming at enhancement of motor recovery. Front Synaptic Neurosci 2018;10:18.
19. Chen C, Ding Q, Shen B, Yu T, Wang H, Xu Y, et al. Insights into the authentic active ingredients and action sites of oral exogenous glutathione in the treatment of ischemic brain injury based on pharmacokinetic-pharmacodynamic studies. Drug Metab Dispos. 2020;48:52–62.
20. Noh JS, Kim EY, Kang JS, Kim HR, Oh YJ, Gwag BJ. Neurotoxic and neuroprotective actions of catecholamines in cortical neurons. Exp Neurol. 1999;159:217–24.
21. Longa EZ, Weinstein PR, Carlson S, Cummins R. Reversible middle cerebral artery occlusion without craniectomy in rats. Stroke. 1989;20:84–91.
22. Yan C, Guo H, Ding Q, Shao Y, Kang D, Yu T, et al. Multiomics profiling reveals protective function of lignans against acetaminophen-induced hepatotoxicity. Drug Metab Dispos. 2020;48:1092–103.
23. Li H, Xiao J, Li X, Chen H, Kang D, Shao Y, et al. Low cerebral exposure cannot hinder the neuroprotective effects of panax notoginsenosides. Drug Metab Dispos. 2018;46:53–65.
24. Lu SC. Glutathione synthesis. Biochim Biophys Acta. 2013;1830:3143–53.
25. Hodgson NW, Waly MI, Trivedi MS, Power-Charnitsky VA, Deth RC. Methylation-related metabolic effects of D4 dopamine receptor expression and activation. Transl Psychiatry. 2019;9:295.
26. Feigin VL, Forouzanfar MH, Krishnamurthi R, Mensah GA, Connor M, Bennett DA, et al. Global and regional burden of stroke during 1990–2010: findings from the global burden of disease study 2010. Lancet. 2014;383:245–54.
27. Gori AM, Giusti B, Piccardi B, Nencini P, Palumbo V, Nesi M, et al. Inflammatory and metalloproteinases profiles predict three-month poor outcomes in ischemic stroke treated with thrombolysis. J Cereb Blood Flow Metab. 2017;37:3253–61.
28. Shih YY, Huang S, Chen YY, Lai HY, Kao YC, Du F, et al. Imaging neurovascular function and functional recovery after stroke in the rat striatum using forepaw stimulation. J Cereb Blood Flow Metab. 2014;34:1483–92.
29. Rice ME, Patel JC, Cragg SJ. Dopamine release in the basal ganglia. Neuroscience. 2011;198:112–37.
30. Bhakta BB, Hartley S, Holloway I, Couzens JA, Ford GA, Meads D, et al. The DARS (dopamine augmented rehabilitation in stroke) trial: protocol for a randomised controlled trial of co-careldopa treatment in addition to routine NHS occupational and physical therapy after stroke. Trials. 2014;15:316.
31. Li P, Stetler RA, Leak RK, Shi Y, Li Y, Yu W, et al. Oxidative stress and DNA damage after cerebral ischemia: potential therapeutic targets to repair the genome and improve stroke recovery. Neuropharmacology. 2018;134:208–17.